

# Design of Two Optimized Controllers of a Hydraulic Actuator Semi-Active Suspension

## A Comparison Study

Saad Babesse

Department of Electrical Engineering,  
Ferhat Abbas University Setif I,  
Setif, Algeria  
saad.babesse@univ-setif.dz

**Abstract**—A parallel optimization of Proportional, Integral and Derivative (PID) controller and a sixth order phase lead-lag compensator of a high order naturally oscillatory hydraulic actuator are proposed in this paper. The PID controller parameters (proportional, integral and derivative) and the compensator parameters (gain, poles and zeros) are obtained by minimizing the Integral of Time Absolute Error (ITAE) criterion. The proposed methods are demonstrated through a realistic numerical synthesis example of a hydraulic actuator dedicated to a semi-active suspension modeled by an eighth order transfer function. A simulation comparison is investigated for both controllers to compare their performances.

**Keywords**—parallel PID; phase lead lag compensator; hydraulic actuator; ITAE

### I. INTRODUCTION

The PID controller has been widely used since its invention [1]. It is a simple and easy way to tune control structures. Since many control systems using PID control are proven to be satisfactory, it still has a wide range of applications in industrial control. In 1989, more than 90% of the control loops were of the PID type [2, 3]. However, most of the classical methods for PID control design suffer from usability restrictions. This may be caused by many reasons such as character of the plant (regarding zeros and poles character and position) or its order [4]. In this paper, we achieve the optimization of the PID parameters with the effective application of integral criterion (ITAE) as an objective function. On the other hand, with the powerful tools provided by Matlab, many optimal control problems can be converted into conventional optimization problems. With the above-mentioned function, some optimal controller problems can be easily solved. Although not allowing elegant analytical solutions, numerical methods are extremely powerful practical techniques for controller design. In this context, a sixth order phase lead-lag compensator based on ITAE criterion minimization was designed and a comparison study between the two previous controllers through a realistic numerical example was conducted, based on time performances such as settling time, response time, and overshoot.

### II. BACKGROUND

There are many PID control configurations, but the most common implementation of this controller is the feedback-loop with a single input and a single output [5] (Figure 1). The typical structure of the PID controller is shown in Figure 2. The signal error  $e(t)$  enters the PID control block and the resulting excitation signal is the sum of the error signal affected by the proportional, integral and derivative actions.

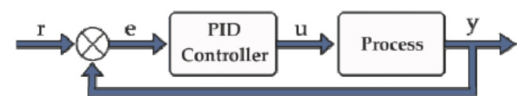


Fig. 1. Block diagram of the simplest PID controller.

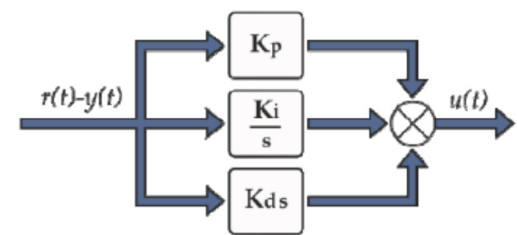


Fig. 2. Block diagram of the typical structure of PID controller.

A Simulink model for the PID control, with ITAE descriptions, is established as shown in Figure 3, where the variable names to be optimized are  $K_p$ ,  $K_i$ ,  $K_d$  and the objective function is the ITAE criterion. In Figure 4, an optimal controller design is explored to calculate the gain, poles and zeros of the desired phase lead lag compensator by reducing the objective function (ITAE criterion) [5]. For both controllers, MATLAB function *fmincon* can be used to solve the constrained optimization problems.

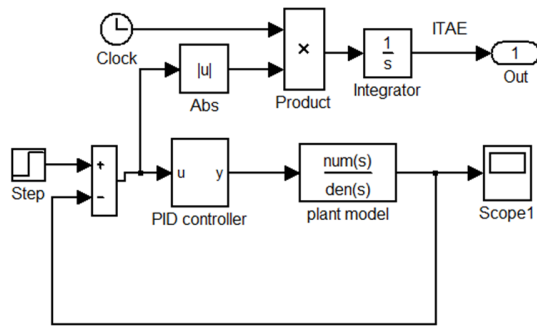


Fig. 3. Simulink model of optimized PID based on ITAE criterion.

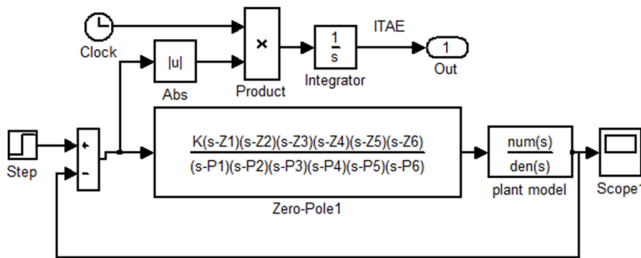


Fig. 4. Simulink model of optimized compensator based on ITAE criterion.

III. NUMERICAL EXAMPLE

Considering the studied Single Input Single Output (SISO) high order system as a hydraulic actuator dedicated to a heavy vehicle anti-roll bar mechanism which has a seven order transfer function, and by adding a first order lead-lag pre-filter, the overall system becomes with an eight order transfer function. A CAD model [7] of one axle fitted with active components can be seen in [6]. The roll plane model of the truck is described in [8, 9]. The truck body (referred to as the ‘sprung mass’) is connected to the suspension trailing arms and axles (referred to as ‘unsprung masses’) by dampers and springs representing the suspension stiffness and damping. The damping has been assumed to be linear and tyre compliance (and therefore roll angle contribution) has been neglected. The suspension consists of two trailing arms free to rotate about their axis independently of each other. Each end of the anti-roll bar is attached to one trailing arm whose position is determined by the wheels and actuator positions. The actuators are mounted between the anti-roll bar and the frame of the trailer. By extending one actuator and retracting the other, the anti-roll bar is twisted and torque is provided to counteract the moment generated by the lateral acceleration and tilt the vehicle into the turn. The different transfer functions are given below [6, 7].

The transfer function between the displacement transducer extension  $x$  and the actuator extension  $y_a$  is given by:

$$\bar{x} = \frac{L}{d_a (I_p + I_{arb})s^2 + 2C d_T d_d s + 2k_s d_s d_T + K_{arb} - mgh} \frac{I_{arb} s^2 + K_{arb}}{F_c h L} \bar{y}_a \quad (1)$$

The transfer function between the actuator extension  $y_a$  and the servo-valve spool displacement  $x_p$  is given by:

$$y_a = \frac{K_x / A_p}{a_{11} s^3 + a_{12} s^2 + a_{13} s + a_{14}} \cdot x_p \quad (2)$$

with:

$$a_{11} = \frac{V_t M_t}{4\beta_e A_p^2}, a_{12} = \left( \frac{K_{pe} M_t}{A_p^2} + \frac{V_t B_p}{4\beta_e A_p^2} \right),$$

$$a_{13} = \left( 1 + \frac{K_{pe} B_p}{A_p^2} + \frac{V_t K_h}{4\beta_e A_p^2} \right), a_{14} = \frac{K_{pe} K_h}{A_p^2}$$

The servo-valve is modeled as a second order Butterworth filter. It is a low-pass filter with a cut-off frequency of 15Hz, which is given by:

$$BW(s) = \frac{\omega_c^2 (\alpha^2 + \beta^2)}{s^2 + 2\alpha\omega_c s + \omega_c^2 (\alpha^2 + \beta^2)} \quad (3)$$

where:  $\omega_c = 30\pi$ .rad/sec,  $\alpha = 0.5949$ , and  $\beta = 0.2830$ .

To keep the entire system stable with the range of given references, we add a lead-lag pre-filter, given by:

$$PF(s) = \frac{\tau_1 s + 1}{\tau_2 s + 1} \quad (4)$$

$\tau_1, \tau_2$  were chosen to enable a reasonable choice of the regulator parameters:  $\tau_1 = 0.001$  s,  $\tau_2 = 2$  s.

The open loop transfer function of the overall system is given by the following transfer function:

$$G(s) = \frac{b_3 s^3 + b_2 s^2 + b_1 s + b_0}{s^8 + a_7 s^7 + a_6 s^6 + a_5 s^5 + a_4 s^4 + a_3 s^3 + a_2 s^2 + a_1 s + a_0} \quad (5)$$

where:

$$b_3 = 1.135 \cdot 10^4, b_2 = 1.135 \cdot 10^7, b_1 = 1.897 \cdot 10^9$$

$$b_0 = 1.897 \cdot 10^{12}, a_7 = 122.1, a_6 = 2.175 \cdot 10^5$$

$$a_5 = 2.421 \cdot 10^7, a_4 = 8.836 \cdot 10^8, a_3 = 4.288 \cdot 10^9$$

$$a_2 = 1.046 \cdot 10^{11}, a_1 = 1.167 \cdot 10^{11}, a_0 = 3.271 \cdot 10^{10}$$

This plant has uncontrollable modes, since:

$$rank(A) = 8, rank(C) = 3$$

(A, B) are extracted from the state space representation of the plant  $G$  and  $C = ctrb(A, B)$  is the controllability matrix. This property can make control difficulties, presented as oscillations in the response.

To design the two controllers, we adopt the following time specifications: Settling time: less than 4s, Rise time: less than 2.5s, and Overshoot%: less than 5%.

A. Optimized PID Based on ITAE Criterion

Using the Matlab function *fmincon* with PID parameters initialization:  $x_{\sigma} = [0.001; 0.001; 0.001]$ , minimization of the objective function ITAE, and after 80 iterations, the solution is [10, 11]:

$$k_p = 0.0288, k_i = 0.0090, k_d = 0.0112$$

**B. Optimized Compensator Based on ITAE Criterion**

The previous Matlab function is used with gain, poles and zeros initialization, and the optimal compensator is obtained by minimising the ITAE criterion. The order of the compensator is chosen after several trial-and-error designs. The best obtained is a sixth order phase lead lag compensator. After 51 iterations, the compensator parameters are obtained as follows:

The gain is:  $K=0.003667$ .

The zeros are:  $Z_1=-0.5887$ ,  $Z_2=-0.5347$ ,  $Z_{3,4}=2.9765\pm 11.8634j$ ,  $Z_{5,6}=6.9850\times 10^{-3}\pm 4.2237\times 10^2j$ .

The poles are:  $P_1=-2.34$ ,  $P_2=-5.768\times 10^{-7}$ ,  $P_{3,4}=-1.2615\pm 2.5105j$ ,  $P_{5,6}=-1.2280\times 10^{-9}\pm 4.0890\times 10^2j$ .

**C. Simulations**

First, we compare the performance of the designed controllers with [7]. The PID controller gains found are:

$$K_p = 0.05; K_i = 0.03; K_d = 2.10^{-3}$$

And then, we apply the different controllers to track the set-point (roll angle) as the input of the hydraulic actuator. We choose as simulation time:  $t_s=20s$ , and the step function as a set-point.

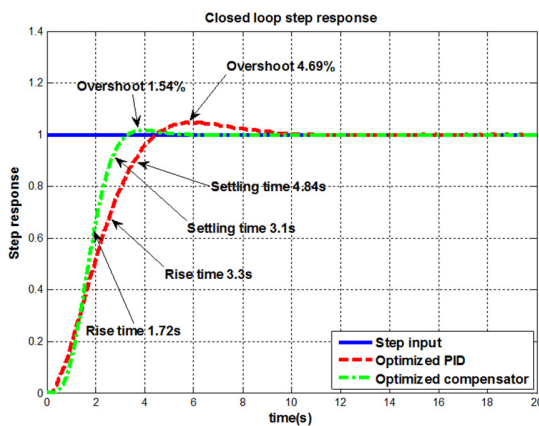


Fig. 5. Time characteristics of optimized controllers closed loop step response.

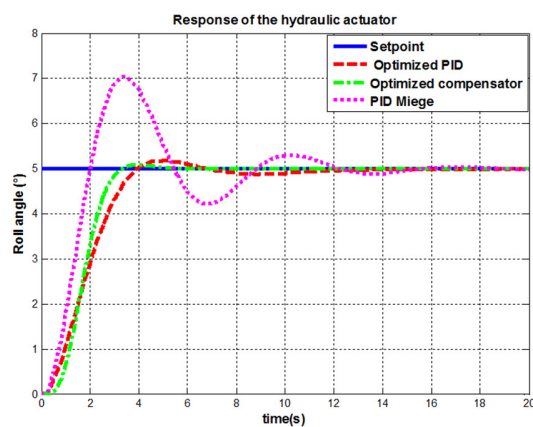


Fig. 6. Response of the hydraulic actuator.

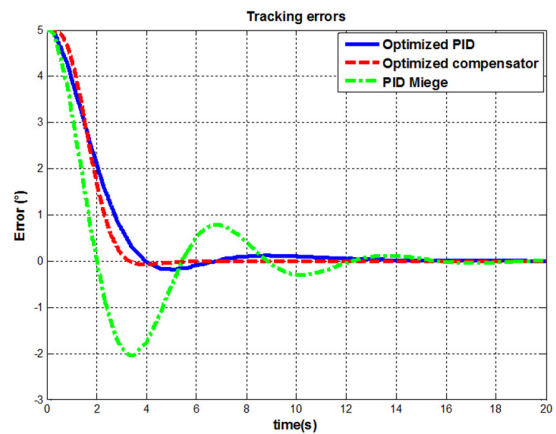


Fig. 7. Tracking errors.

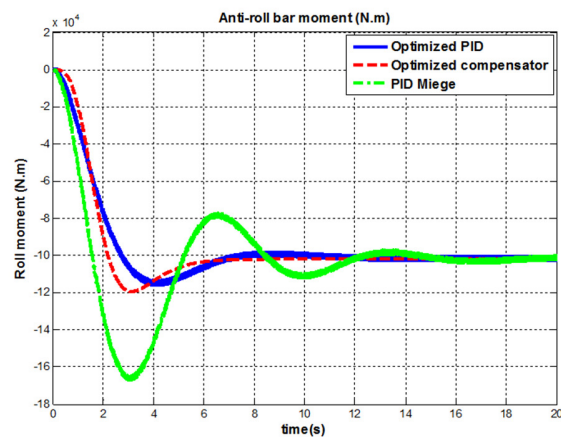


Fig. 8. Generated anti-roll bar moment.

Figure 5 shows that all time characteristics (overshoot%, rise time and settling time) of the optimized compensator are better than those of the optimized PID. In Figure 6, the response of the hydraulic actuator to  $5^\circ$  roll angle setpoint gives good tracking and less overshoot in the optimized compensator case comparing it with optimized PID and that of [7]. This can also be expressed by the errors shown in Figure 7. The response of the PID controller of [7] gave oscillations and an overshoot of 40%. The required roll moment generated by the antiroll bar is shown in Figure 8. One can see that the maximum moment is towards  $-11.8\times 10^4 N.m$  in the case of the optimized compensator and  $-11.2\times 10^4 N.m$  for the optimized PID and  $-16.4\times 10^4 N.m$  for the PID case of [7] (these values must be less than the maximum tolerated moment of the actuator). Sign (-) indicates that the roll moment and the roll angle are in opposite directions.

Now, we apply a variable setpoint to the three controllers, and then we compare their behaviors. Figures 9-10 show that the controllers track the variable setpoint plant with fast response of the optimized compensator comparing it with optimized PID. But the oscillations always persist for the PID case of [7].

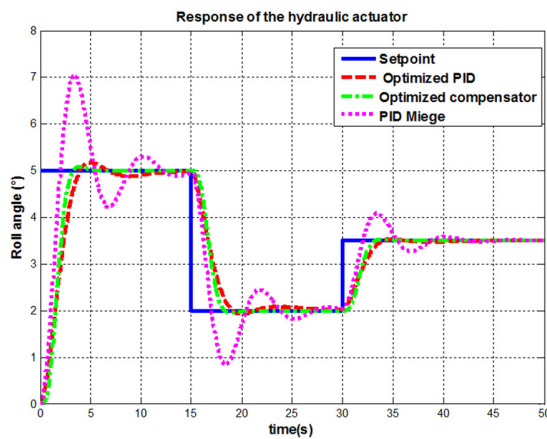


Fig. 9. Response of the hydraulic actuator.

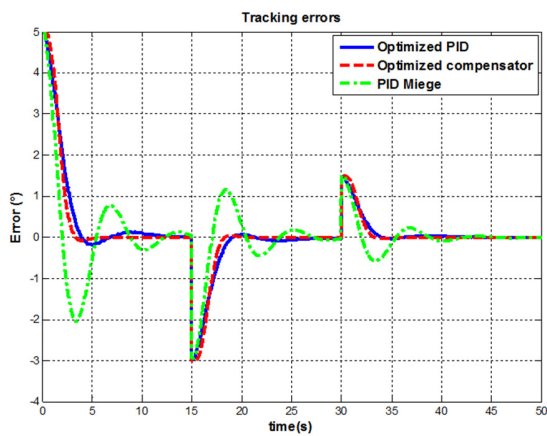


Fig. 10. Tracking errors.

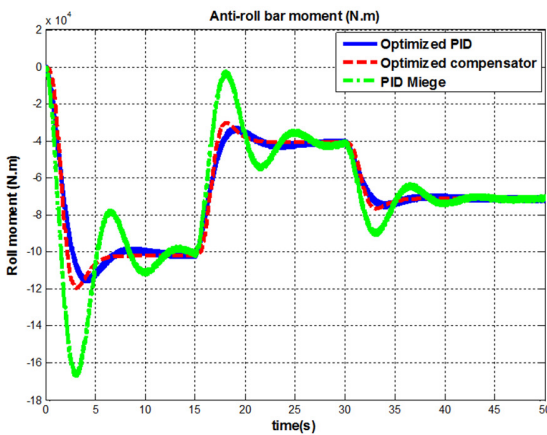


Fig. 11. Generated anti-roll bar moment.

The optimized compensator requires an antiroll moment greater than that of the optimized PID, but less than the maximum tolerated roll moment of the antiroll bar mechanism, as shown in Figure 11. The comparison between the different time characteristics of the proposed controllers is summarized in Table I.

TABLE I. COMPARISON OF THE CONTROLLERS PERFORMANCES

Controller	Time characteristics		
	Overshoot (%)	Rise time (s)	Settling time (s)
Optimized PID	4.69	3.3	4.34
Optimized compensator	1.54	1.72	3.1
[7]	40.9	1.47	10.92

TABLE II. ANTIROLL BAR PARAMETERS

Parameter	Description	Value
$\beta_e (N/m^2)$	Effective bulk modulus of hydraulic oil	$6.89 \times 10^6$
$A_p (m^2)$	Area of piston of hydraulic actuator	0.0123
$C (Ns/m^2)$	Damping force coefficient	10000
$d_a (m)$	Distance to the actuator from the centreline of suspension	0.215
$d_d (m)$	Distance to damper from centreline of suspension	0.23
$d_s (m)$	Distance to air spring from centreline of suspension	0.535
$d_T (m)$	Half track width	0.93
$I_{arb} (Kg.m^2)$	Moment of inertia of anti-roll bar about roll centre of suspension	6.10
$I_p (Kg.m^2)$	Moment of inertia of sprung mass about roll center of suspension	9500
$k_s (N/m)$	Air spring stiffness	$2.37 \times 10^5$
$k_{arb} (Nm/rad)$	Roll stiffness of anti-roll bar	$1.02 \times 10^6$
$k_h \left( \frac{N}{m \cdot rad} \right)$	Spring stiffness in Merritt's valve-piston model	$1.1033 \times 10^7$
$k_{pe} \left( \frac{m^3/s}{N/m^2} \right)$	Servo-valve total flow pressure coefficient	$4.2 \times 10^{-11}$
$k_x \left( \frac{m^3/s}{m} \right)$	Servo-valve flow gain coefficient	2.5
$L (m)$	Distance to displacement transducer from centreline of suspension	0.552
$M_t (kg)$	Mass of load in Merritt's valve-piston model	65.9816
$B_p \left( \left( \frac{kg \cdot N}{m \cdot rad} \right)^{0.5} \right)$	Damping coefficient in Merritt's valve-piston model	539.6201
$P_s (bar)$	Supply pressure of hydraulic system	210
$V_t (m^3)$	Volume of 'trapped' oil at high pressure in the hydraulic system	0.0014

IV. CONCLUSION

Two optimized controllers based on integral time absolute error minimization criterion and utilizing Matlab/Simulink are proposed. It was shown that the optimized compensator gives better time characteristics performances than the optimized PID and PID based on root locus method. A simulation comparison, using step set-point and variable set-point, was investigated. The optimized compensator presented in this work can enhance considerably the control of this type of antiroll bar mechanisms mounted on experimental and real trucks

REFERENCES

- [1] A. Firoozshahi, "Innovative Tank Management System based on DCS", IEEE, ELMAR 2010, Zadar, Croatia, September 15-17, 2010
- [2] C. C. Yu, Autotuning of PID Controllers: Relay Feedback Approach, Springer-Verlag, 1999
- [3] K. J. Astrom, T. Hagglund, Automatic Tuning of PID Controllers, Instrument Society of America, 1988

- 
- [4] S. Ozana, T. Docekal, "PID controller design based on global optimization technique with additional constraints", *Journal of Electrical Engineering*, Vol. 67, No. 3, pp. 160-168, 2016
- [5] M. Milosawlewitsch-Aliaga, R. A. Osornio-Rios, R. J. Romero-Troncoso, "Model-Based Iterative Feedback Tuning for Industrial PID Controllers", *Journal of Scientific and Industrial Research*, Vol. 69, No. 12, pp. 930-936, 2010
- [6] D. J. M. Sampson, P. G. McKeivitt, D. Cebon, "The development of an active roll control system for heavy vehicles", *16<sup>th</sup> IAVSD Symposium on the Dynamics of Vehicles on Roads and Tracks*, Pretoria, South Africa, 1999
- [7] A. J. P. Miede, *Development of Active Anti-Roll Control for Heavy Vehicles, First Year Report Submitted to the University of Cambridge*, University of Cambridge, 2000
- [8] S. Babesse, D. Ameddah, F. Inel, "Comparison between RST and PID Controllers Performance of a Reduced Order Model and the Original Model of a Hydraulic Actuator dedicated to a Semi-active Suspension", *World Journal of Engineering*, Vol. 13, No. 1, pp. 66-71, 2016
- [9] S. Babesse, D. Ameddah, "Neuronal active anti-roll control of a single unit heavy vehicle associated with RST control of the hydraulic actuator", *International Journal of Heavy Vehicle Systems*, Vol. 22, No. 3, pp. 236-254, 2015
- [10] R. A. Waltz, J. L. Morales, J. Nocedal, D. Orban, "An interior algorithm for nonlinear optimization that combines line search and trust region steps", *Mathematical Programming*, Vol. 107, No. 3, pp. 391-408, 2006
- [11] T. K. Kiong, W. Qing-Guo, H. C. Chieh, T. J. Hagglund, *Advances in PID Control*, Springer Verlag, 2000